IET Communications

Research Article

IET Journals
The Institution of Engineering and Technology

Equalisation, despreading, and beamforming scenarios of complex spread-OFDM/OQAM in single-input multi-output channels

ISSN 1751-8628
Received on 23rd June 2018
Revised 3rd December 2018
Accepted on 16th January 2019
E-First on 19th March 2019
doi: 10.1049/iet-com.2018.5581
www.ietdl.org

Seyyed Mohammad Javad Asgari Tabatabaee[1] ✉, *Mohammad Towliat*[2], *Morteza Rajabzadeh*[3]

[1]*Department of Electrical Engineering, University of Torbat Heydarieh, Torbat Heydarieh, Iran*
[2]*Department of Electrical Engineering, Ferdowsi University of Mashhad, Mashhad 9177948974, Iran*
[3]*Electrical Engineering Department, Quchan University of Technology, Quchan, Khorasan Razavi, 9471784686, Iran*
✉ *E-mail: s.m.j.asgaritabatabaee@torbath.ac.ir*

Abstract: Orthogonal frequency division multiplexing/offset quadrature amplitude modulation (OFDM/OQAM) is a promising multicarrier system, which can achieve a better bandwidth efficiency than cyclic prefix (CP)-OFDM. However, OFDM/OQAM suffers from an inherent interference. Since in OFDM/OQAM, the data symbols are real-valued, the pure imaginary self-interference can be eliminated by removing the imaginary part of the received signal. On the other hand, in the literature, it is shown that even for complex-valued data symbols, the self-interference can be eliminated if a spreading code is employed. The resulted scheme is called spread-OFDM/OQAM. In this study, we extend spread-OFDM/OQAM for single-input multi-output channels. In case of multiple antennas, at the receiver after demodulation, the following processes must be performed: equalisation (to remove the channel effect), despreading of spreaded symbols, and beamforming of multiple antennas. We propose three scenarios to apply the mentioned processes. In the first scenario, despreading, equalisation, and beamforming are performed jointly in one step. In the second scenario, despreading and equalisation are accomplished jointly and then beamforming is performed. In the last scenario, each of those processes is applied separately. We compare the complexity of the proposed approaches. Also their performance is evaluated through simulations in terms of bit error rate.

1 Introduction

In recent years, orthogonal frequency division multiplexing (OFDM) has been the most popular multicarrier technique to compensate for the frequency selectivity of channels due to its simple implementation, good performance and simple adaptation to multiple antennas [1–3]. On the down side, OFDM suffers from some drawbacks making it fall short to fulfil the rising demands of fifth generation (5G) communication networks. Firstly, the large spectral side lobes in the OFDM signal lead to a poor performance in time variant channels or channels with large Doppler shift [4–6]. Furthermore, a cyclic prefix (CP) is appended to each OFDM block to prevent the inter-block-interference, which reduces the bandwidth efficiency [4–7].

OFDM/offset quadrature amplitude modulation(OQAM) is an alternative multicarrier technique, which by using a well-localised prototype filter, shapes the transmitted symbol blocks [8, 9], and can overcome the mentioned drawbacks of OFDM [4–9]. However, OFDM/OQAM suffers from an inherent interference, which appears even in distortion-free channels. This interference is eliminated by transmitting real-valued symbols, instead of complex-valued symbols, and taking the real part of the received signal [4, 10]. On the other hand, transmitting real-valued symbols prevents the application of maximum likelihood detection of space-time coding in multi-input multi-output (MIMO) OFDM/OQAM scenarios [4, 11, 12]. Hence, transmitting complex-valued symbols, instead of real-valued ones, is proposed to address these concerns in MIMO OFDM/OQAM [13–16]. However, eliminating the interference among the complex-valued symbols requires some innovative techniques.

In [14], the authors show that if spread spectrum coding is combined with OFDM/OQAM, the inherent interference can be completely removed without requiring the data symbols to be real-valued. This system is called spread-OFDM/OQAM. At the transmitter of spread-OFDM/OQAM, firstly, data symbols are spread by using a well-chosen Walsh–Hadamard code and then, the coded signal is modulated by the conventional OFDM/OQAM. At the receiver side, first of all, the received signal is demodulated. Then, a one-tap equaliser is used at each subcarrier, in order to compensate for the effect of the channel (the most challenging part of the OFDM/OQAM transceiver is the design of the equaliser [17–20]). Finally, the coded symbols are despread. Based on the developed technique in [14], for spread-OFDM/OQAM, a new equalisation and despreading method was proposed in [16]. In this method, equalisation and despreading are applied jointly in order to maximise the signal to interference plus noise ratio (SINR) for each data symbol.

On the other hand, it is well known that by using multiple antennas at the transmitter and receiver, spatial diversity is achieved, which improves the communication system performance. Accordingly, using MIMO techniques is known as a promising method for future communication networks [21, 22]. In the case of multiple antennas, beamforming is known as an efficient technique to achieve full spatial diversity [23, 24]. To our best knowledge, to extract the channel spatial diversity, the combination of beamforming techniques and spread-OFDM/OQAM is not reported in the literature so far.

In this study, we propose three different methods in order to apply beamforming techniques in spread-OFDM/OQAM systems when multiple antennas are used at the receiver. In this regard, by using the proposed beamforming methods, in addition to overcoming OFDM drawbacks, we can benefit the spatial diversity to improve the performance. It must be noted that the spreading code is just used to eliminate the inherent interference of OFDM/OQAM, and the communication system is considered a single user in this study. For the considered spread-OFDM/OQAM system in a single-input multi-output (SIMO) channel, after demodulation at each receiver antenna, the following processes must be performed: equalisation, despreading, and beamforming. We propose three scenarios for implementing the above-mentioned processes. In the first scenario (S1), all tasks are jointly performed. In S1, based on the SINR maximisation for each data symbol, an estimation vector is obtained, which is applied on the demodulated symbols of all subcarriers and all antennas in order to estimate data symbols at a single step. In order to reduce computational complexity, in the second scenario (S2), those three processes are performed at two

separate steps. Firstly, equalisation and despreading are performed jointly and after that in the second step, beamforming is performed. Similar to S1, the operator vectors of the two steps are obtained based on the SINR maximisation in S2. In the third scenario (S3), equalisation, despreading, and beamforming are performed separately. In S3, equalisation is performed at each subchannel, individually. Moreover, the spreading code (which is used in the transmitter) is applied at the receiver to despread data symbols. Intuitively, S3 has the lowest computational complexity because of separate operations. In this study, we compare the computational complexity order of the three proposed scenarios and also evaluate their performance in terms of bit error rate (BER) through simulations. All in all, the contributions of this work can be summarised as follows:

- Extending spread-OFDM/OQAM to SIMO channels and applying beamforming to achieve receiver diversity.
- Proposing three equalisation, despreading, and beamforming methods at the receiver in order to remove interference of spread-OFDM/OQAM in SIMO channels.
- Comparing the computational complexity of the proposed three methods.
- Evaluating the performance of the proposed methods through simulations.

The remaining part of this paper is structured as follows. In the next section, we present the model of the spread-OFDM/OQAM system proposed in [14, 16]. In Section 3, we extend spread-OFDM/OQAM to SIMO channels and propose three scenarios for equalisation, despreading, and beamforming at the receiver after demodulation. We compare the computational complexity order of the proposed scenarios in Section 4 and in Section 5 the performance of these methods are evaluated through simulations. Finally, we conclude this paper in Section 6.

2 Spread-OFDM/OQAM system model

Assume that the prototype filter $g(t)$ is used in OFDM/OQAM to transmit the data symbols. The transmitter sends the data symbols on M subcarriers as follows:

$$s(t) = \sum_{n=-\infty}^{+\infty} \sum_{m=0}^{M-1} a_{m,n} g_{m,n}(t), \tag{1}$$

where $a_{m,n}$ is the complex-valued symbol transmitted at the mth subcarrier and nth time instant. $g_{m,n}(t) \triangleq g(t - nT_0)\mathrm{e}^{\mathrm{j}2\pi mF_0 t}\varphi_{m,n}$ is the shifted version of prototype filter $g(t)$ in time and frequency with steps nT_0 and mF_0, respectively. Also, $\varphi_{m,n}$ is a staggered factor defined as $\varphi_{m,n} \triangleq (-1)^{mn}\mathrm{j}^{m+n}$. In OFDM/OQAM (which achieves maximal symbol density between filter bank multicarrier systems [11]), $F_0T_0 = 0.5$ and data symbols are real valued.

Let us denote the received signal by $y(t)$. In order to demodulate the transmitted symbol at the m_0th subcarrier in the n_0th time instant (i.e. a_{m_0,n_0}), filtering and sampling are performed at the receiver as

$$y_{m_0,n_0} = \left\langle y(t), g_{m_0,n_0}(t)\right\rangle = \int_{-\infty}^{+\infty} y(t) g^*_{m_0,n_0}(t)\mathrm{d}t\,. \tag{2}$$

If the channel is ideal and there is no noise, then $y(t) = s(t)$. Therefore, by using (1), (2) can be rewritten as

$$y_{m_0,n_0} = \left\langle s(t), g_{m_0,n_0}(t)\right\rangle = a_{m_0,n_0}\left\langle g_{m_0,n_0}(t), g_{m_0,n_0}(t)\right\rangle + \sum_{\substack{m=-\Delta_m \\ m\neq 0}}^{\Delta_m} \sum_{\substack{n=-\Delta_n \\ n\neq 0}}^{\Delta_n} a_{m_0+m,n_0+n}\left\langle g_{m_0+m,n_0+n}(t), g_{m_0,n_0}(t)\right\rangle, \tag{3}$$

where Δ_m and Δ_n are the ranges for $|m| > \Delta_m$ or $|n| > \Delta_n$, the time and frequency interferences of the symbols at the vicinity of a_{m_0,n_0} are approximately and can be ignored ($\left\langle g_{m_0+m,n_0+n}(t), g_{m_0,n_0}(t) = 0\right\rangle$). As can be seen, the demodulated symbol includes two parts. The first part contains the desired symbol and the second part contributes to the interference generated by other symbols on the desired symbol. According to (3), the interference term appears even if the channel is ideal and, as a result, it is known as the inherent interference in OFDM/OQAM. In [4], it is shown that if real-valued symbols are transmitted and the prototype filter satisfies a specific condition (which is called real orthogonality), the inherent interference is a pure imaginary term and it can be removed by taking the real part of y_{m_0,n_0}. On the other side, if the channel is not ideal (but can be assumed flat through overlapped subcarriers), the interference can be eliminated by applying a simple one-tap equalieer before the real-taking operation [4]. Although this technique effectively works in single-input single-output (SISO) channels, it can lead to a significant degradation of performance in MIMO channels [14].

In [14], it is shown if spread spectrum coding is combined with OFDM/OQAM transmitting complex symbols, without real-taking operation at the receiver, the interference can be perfectly eliminated. Note that in such a system, the spread spectrum code is not used for sending the data of multiple users but is used to spread the data symbols of a single user on all subcarriers of the OFDM/OQAM transceiver. In order to present the proposed work in [14] for the single user system, we express the demodulated symbols of all subcarriers at the n_0th time instant in vector form as (see (3))

$$\boldsymbol{y}_{n_0} = \boldsymbol{G}_0\boldsymbol{a}_{n_0} + \sum_{\substack{n=-\Delta_n \\ n\neq 0}}^{\Delta_n} \boldsymbol{G}_n\boldsymbol{a}_{n_0+n}, \tag{4}$$

where $\boldsymbol{y}_n \triangleq [y_{0,n} \quad \cdots \quad y_{M-1,n}]^{\mathrm{T}}$ is the vector of demodulated symbols at the nth time instant and $\boldsymbol{a}_n \triangleq [a_{0,n} \quad \cdots \quad a_{M-1,n}]^{\mathrm{T}}$ is the vector of transmitted complex-valued symbols at the nth time instant. Also, $\boldsymbol{G}_n$ is a $M \times M$ matrix whose (i,j)th entry is obtained as $g_n^{i,j} = \left\langle g_{i,n_0+n}(t), g_{j,n_0}(t)\right\rangle$. In order to combine the OFDM/OQAM system with spread spectrum coding, a well-chosen code must be employed [14]. Assume that $\boldsymbol{c}_u \triangleq [c_{0,u} \ldots c_{M-1,u}]^{\mathrm{T}}$ is the spreading code with the length of M (equal to the number of subcarriers), which is applied to spread the uth data symbol. The matrix $\boldsymbol{C} \triangleq [\boldsymbol{c}_1 \quad \ldots \quad \boldsymbol{c}_U]$ with the size of $M \times U$ includes spreading codes of all data symbols (the number of all data symbols is U). Note that in this study, in order to maximise the bandwidth efficiency, we consider that $U = M/2$ [14]. Assume that $d_{n,u}$ is the uth complex symbol at the nth time instant, which must be spread on all subcarriers. As a result, $\boldsymbol{a}_n = \boldsymbol{C}\boldsymbol{d}_n$, where $\boldsymbol{d}_n \triangleq [d_{n,1} \quad \ldots \quad d_{n,U}]^{\mathrm{T}}$ contains all data symbols at the nth time instant. Thus, (4) can be rewritten as

$$\boldsymbol{y}_{n_0} = \boldsymbol{G}_0\boldsymbol{C}\boldsymbol{d}_{n_0} + \sum_{\substack{n=-\Delta_n \\ n\neq 0}}^{\Delta_n} \boldsymbol{G}_n\boldsymbol{C}\boldsymbol{d}_{n_0+n}\,. \tag{5}$$

At the receiver, after demodulation, despreading is performed as

$$\boldsymbol{z}_{n_0} = \boldsymbol{C}^{\mathrm{T}}\boldsymbol{y}_{n_0} = \boldsymbol{C}^{\mathrm{T}}\boldsymbol{G}_0\boldsymbol{C}\boldsymbol{d}_{n_0} + \sum_{\substack{n=-\Delta_n \\ n\neq 0}}^{\Delta_n} \boldsymbol{C}^{\mathrm{T}}\boldsymbol{G}_n\boldsymbol{C}\boldsymbol{d}_{n_0+n}, \tag{6}$$

where $\boldsymbol{z}_{n_0} \triangleq [z_{n_0,1} \quad \ldots \quad z_{n_0,U}]^{\mathrm{T}}$ is the decoded symbol vector containing all estimated data symbols at the n_0th time instant. As shown in [14], if $\boldsymbol{C}$ is a well-chosen Walsh–Hadamard code and $U \leq M/2$, then

$$\boldsymbol{C}^{\mathrm{T}}\boldsymbol{G}_n\boldsymbol{C} = \begin{cases} \boldsymbol{I}_U, & \text{when } n = 0, \\ \boldsymbol{0}_U, & \text{when } n \neq 0, \end{cases} \tag{7}$$

where $\mathbf{0}_U$ is a zero matrix with size $U \times U$. By replacing (7) into (6), we have $\boldsymbol{z}_{n_0} = \boldsymbol{d}_{n_0}$, which means that the desired symbols are obtained without any interference. Furthermore, if the channel is not ideal, but it can be assumed flat and time invariant through overlapped adjacent time instants and subcarriers, by using a simple one-tap equaliser before despreading, the channel effect can be properly eliminated. Although this method has a good BER performance in low-frequency selective channels, in some high-frequency selective channels, where the spectrum cannot be assumed flat over overlapped pulses, the performance of this method dramatically degrades [16]. We have previously proposed a new method in [16], in which despreading and equalisation are performed jointly with good performance even in very high frequency selective SISO channels. This method is elaborated in the following.

Assume that the transmitted signal passes through a communication channel with impulse response $h(t)$ and is added with a white Gaussian noise $v(t)$. Therefore, the input signal of the receiver can be expressed with

$$\begin{aligned} y(t) &= \int_{-\infty}^{+\infty} h(\tau)s(t-\tau)\,\mathrm{d}\tau + v(t) \\ &= \sum_{m=0}^{M-1}\sum_{n} a_{m,n}g_{m,n}^{(h)}(t) + v(t), \end{aligned} \tag{8}$$

where $g_{m,n}^{(h)}(t) = \int_{-\infty}^{+\infty} h(\tau)g_{m,n}(t-\tau)\,\mathrm{d}\tau$. By considering (8), in case of non-ideal channel, (5) can be replaced as

$$\boldsymbol{y}_{n_0} = \boldsymbol{G}_0^{(h)}\boldsymbol{C}\boldsymbol{d}_{n_0} + \sum_{\substack{n=-\Delta_n \\ n\neq 0}}^{\Delta_n} \boldsymbol{G}_n^{(h)}\boldsymbol{C}\boldsymbol{d}_{n_0+n} + \boldsymbol{v}_{n_0}, \tag{9}$$

where $\boldsymbol{G}_n^{(h)}$ is an $M \times M$ matrix whose (i,j)th entry is $g_n^{(h)\,i,j} \triangleq \left\langle g_{i,n_0+n}^{(h)}(t), g_{j,n_0}(t)\right\rangle$. Also, $\boldsymbol{v}_{n_0} \triangleq [v_{0,n_0} \dots v_{M-1,n_0}]^{\mathrm{T}}$ is the noise vector. In order to jointly equalise and despread the uth data symbol, the estimation vector $\boldsymbol{f}_u^{(h)}$ is used. In this regard, the u_0th despread data symbol at the n_0th time instant can be presented as [16]

$$\begin{aligned} z_{n_0,u_0} &= \boldsymbol{f}_{u_0}^{(h)\mathrm{H}}\boldsymbol{y}_{n_0} = \boldsymbol{f}_{u_0}^{(h)\mathrm{H}}\boldsymbol{G}_0^{(h)}\boldsymbol{C}\boldsymbol{d}_{n_0} \\ &\quad + \sum_{\substack{n=-\Delta_n \\ n\neq 0}}^{\Delta_n} \boldsymbol{f}_{u_0}^{(h)\mathrm{H}}\boldsymbol{G}_n^{(h)}\boldsymbol{C}\boldsymbol{d}_{n_0+n} + \boldsymbol{f}_{u_0}^{(h)\mathrm{H}}\boldsymbol{v}_{n_0} \\ &= \boldsymbol{f}_{u_0}^{(h)\mathrm{H}}\boldsymbol{G}_0^{(h)}\boldsymbol{c}_{u_0}d_{n_0,u_0} + \boldsymbol{f}_{u_0}^{(h)\mathrm{H}}\boldsymbol{G}_0^{(h)}\sum_{\substack{u=1 \\ u\neq u_0}}^{U}\boldsymbol{c}_u d_{n_0,u} \\ &\quad + \sum_{\substack{n=-\Delta_n \\ n\neq 0}}^{\Delta_n} \boldsymbol{f}_{u_0}^{(h)\mathrm{H}}\boldsymbol{G}_n^{(h)}\boldsymbol{C}\boldsymbol{d}_{n_0+n} + \boldsymbol{f}_{u_0}^{(h)\mathrm{H}}\boldsymbol{v}_{n_0}. \end{aligned} \tag{10}$$

As it can be seen in (10), z_{n_0,u_0} contains four parts. The first part is the desired symbol. The second part contains interference from other data symbols at the n_0th time instant. The third part is the interference of other time instants. Finally, the fourth part indicates the noise effect. In [16], by maximising the signal to noise ratio (SINR) of the u_0th data symbol (for $u_0 = 1, 2, \dots, U$), $\boldsymbol{f}_{u_0}^{(h)}$ is obtained as

$$\boldsymbol{f}_{u_0}^{(h)} = \left(\boldsymbol{A}_{u_0} + \boldsymbol{B}\right)^{-1}\boldsymbol{G}_0^{(h)}\boldsymbol{c}_{u_0}, \tag{11}$$

where

$$\begin{aligned} \boldsymbol{A}_{u_0} &= \boldsymbol{G}_0^{(h)}\left(\sum_{\substack{u=1 \\ u\neq u_0}}^{U}\boldsymbol{c}_u\boldsymbol{c}_u^{\mathrm{T}}\right)\boldsymbol{G}_0^{(h)\mathrm{H}} \\ &\quad + \sum_{\substack{n=-\Delta_n \\ n\neq 0}}^{\Delta_n}\boldsymbol{G}_n^{(h)}\boldsymbol{C}\boldsymbol{C}^{\mathrm{T}}\boldsymbol{G}_n^{(h)\mathrm{H}} \end{aligned} \tag{12}$$

and $\boldsymbol{B} = \mathrm{E}\left[\boldsymbol{v}_{n_0}\boldsymbol{v}_{n_0}^{\mathrm{T}}\right]$ is the $M \times M$ covariance matrix of the noise vector.

In the following section, we extend the proposed method in [14] (which was for SISO channels) to the case, where the number of receiver antennas is more than one (we have SIMO channels). In this regard, in addition to equalisation and despreading, a beamforming approach is needed to obtain the multiple channel diversity gain. In this study, we propose three different solutions for despreading–equalisation–beamforming tasks at the receiver.

3 Spread-OFDM/OQAM in SIMO channels

Consider a complex spread-OFDM/OQAM system in which the transmitter and receiver are equipped with one and N_{R} antennas, respectively (i.e. SIMO channel). Fig. 1 shows the procedure of transmitting symbols through a SIMO channel. The transmitter sends signal as elaborated in (1). $h^l(t)$ is the channel impulse response between the transmitter and the lth receiver antenna. As shown in Fig. 1, at each antenna of the receiver, filtering and sampling are performed. The demodulated symbol vector of the lth antenna in the nth time instant is $\boldsymbol{y}_n^l \triangleq [y_{0,n}^l \quad \dots \quad y_{M-1,n}^l]^{\mathrm{T}}$, where $y_{m,n}^l$ is the demodulated symbol at the lth antenna and the mth subcarrier in the nth time instant. By using (5), $\boldsymbol{y}_{n_0}^l$ can be written as

$$\begin{aligned} \boldsymbol{y}_{n_0}^l &= \boldsymbol{G}_0^{l,(h)}\boldsymbol{C}\boldsymbol{d}_{n_0} \\ &\quad + \sum_{\substack{n=-\Delta_n \\ n\neq 0}}^{\Delta_n}\boldsymbol{G}_n^{l,(h)}\boldsymbol{C}\boldsymbol{d}_{n_0+n} + \boldsymbol{v}_{n_0}^l, \end{aligned} \tag{13}$$

where $\boldsymbol{G}_n^{l,(h)}$ is an $M \times M$ matrix in which the (i,j)th entry is $g_n^{l,(h)\,i,j} \triangleq \left\langle g_{i,n_0+n}^{l,(h)}(t), g_{j,n_0}(t)\right\rangle$ and $g_{m,n}^{l,(h)}(t) = \int_{-\infty}^{+\infty} h^l(\tau)g_{m,n}(t-\tau)\,\mathrm{d}\tau$.

After demodulation at each antenna and subchannel, the data symbols are passed to the estimation phase. In order to estimate the data symbols, the interference must be eliminated. Furthermore, since we are using multiple antennas at the receiver, we can employ beamforming methods to improve the performance. Thus, to exploit data symbols from the demodulated signal in (13), equalisation, despreading, and beamforming are three tasks, which must be carried out.

3.1 S1: joint equalisation–despreading–beamforming

In S1, equalisation, despreading, and beamforming are performed, jointly. Fig. 2 shows the procedure of this scenario at the receiver. Consider vector $\bar{\bar{\boldsymbol{y}}}_n \triangleq [\boldsymbol{y}_n^{1\mathrm{T}} \quad \dots \quad \boldsymbol{y}_n^{N_{\mathrm{R}}\mathrm{T}}]^{\mathrm{T}}$ with the length of MN_{R}, which contains all demodulated symbols of all receiver antennas and all subcarriers at the nth time instant. By considering (13), $\bar{\bar{\boldsymbol{y}}}_{n_0}$ can be written as

$$\bar{\bar{\boldsymbol{y}}}_{n_0} = \bar{\bar{\boldsymbol{G}}}_0^{(h)}\boldsymbol{C}\boldsymbol{d}_{n_0} + \sum_{\substack{n=-\Delta_n \\ n\neq 0}}^{\Delta_n}\bar{\bar{\boldsymbol{G}}}_n^{(h)}\boldsymbol{C}\boldsymbol{d}_{n_0+n} + \bar{\bar{\boldsymbol{v}}}_{n_0}, \tag{14}$$

where

$$\bar{\bar{\boldsymbol{G}}}_n^{(h)} = \begin{bmatrix} \boldsymbol{G}_n^{1,(h)} \\ \vdots \\ \boldsymbol{G}_n^{N_{\mathrm{R}},(h)} \end{bmatrix} \tag{15}$$

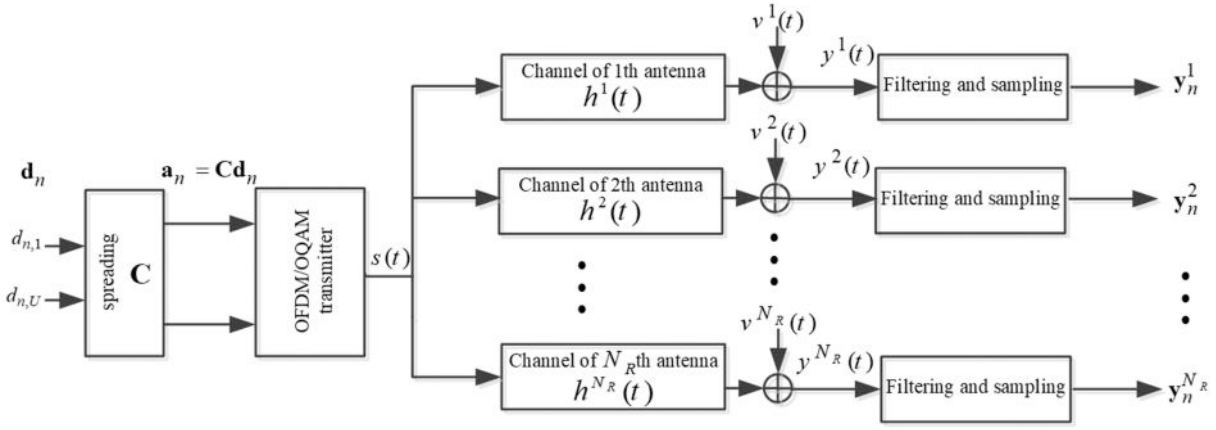

Fig. 1 *Symbol transmission on spread-OFDM/OQAM systems in SIMO channel*

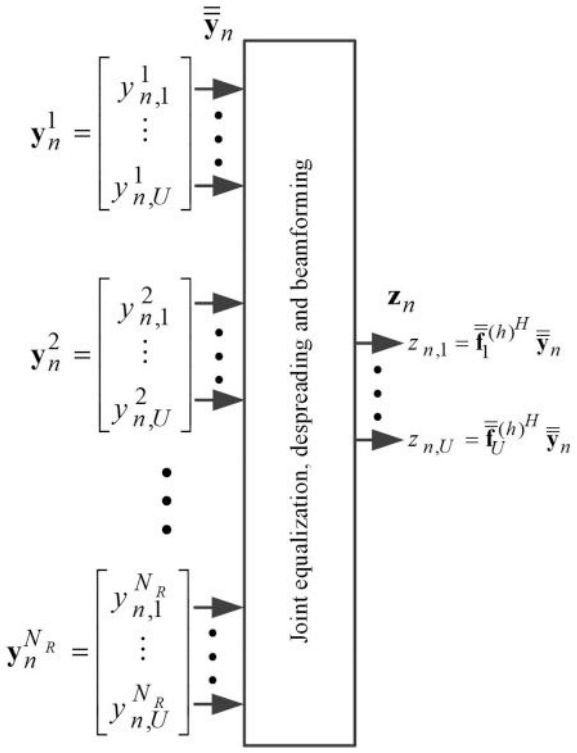

Fig. 2 *S1: joint equalisation–despreading–beamforming at the receiver of spread-OFDM/OQAM in SIMO channels*

is a $MN_{\mathrm{R}} \times U$ matrix and $\bar{\bar{\boldsymbol{v}}}_n \triangleq [\boldsymbol{v}_n^{1\mathrm{T}} \quad \dots \quad \boldsymbol{v}_n^{N_{\mathrm{R}}\mathrm{T}}]^{\mathrm{T}}$ is the noise vector of all antennas and all subcarriers at the nth time instant. In order to develop the joint equalisation–despreading–beamforming method for exploiting the uth data symbol, the vector $\bar{\bar{\boldsymbol{f}}}_u^{(h)}$ with the length of MN_{R} is used. Accordingly, the u_0th estimated symbol at the n_0th time instant can be presented as

$$\begin{aligned} z_{n_0,u_0} &= \bar{\bar{\boldsymbol{f}}}_{u_0}^{(h)\mathrm{H}} \bar{\bar{\boldsymbol{y}}}_{n_0} = \bar{\bar{\boldsymbol{f}}}_{u_0}^{(h)\mathrm{H}} \bar{\bar{\boldsymbol{G}}}_0^{(h)} \boldsymbol{C}\boldsymbol{d}_{n_0} \\ &\quad + \sum_{\substack{n=-\Delta_n \\ n\neq 0}}^{\Delta_n} \bar{\bar{\boldsymbol{f}}}_{u_0}^{(h)\mathrm{H}} \bar{\bar{\boldsymbol{G}}}_n^{(h)} \boldsymbol{C}\boldsymbol{d}_{n_0+n} + \bar{\bar{\boldsymbol{f}}}_{u_0}^{(h)\mathrm{H}} \bar{\bar{\boldsymbol{v}}}_{n_0} \\ &= \bar{\bar{\boldsymbol{f}}}_{u_0}^{(h)\mathrm{H}} \bar{\bar{\boldsymbol{G}}}_0^{(h)} \boldsymbol{c}_{u_0} d_{n_0,u_0} + \bar{\bar{\boldsymbol{f}}}_{u_0}^{(h)\mathrm{H}} \bar{\bar{\boldsymbol{G}}}_0^{(h)} \sum_{\substack{u=1 \\ u\neq u_0}}^{U} \boldsymbol{c}_u d_{n_0,u} \\ &\quad + \sum_{\substack{n=-\Delta_n \\ n\neq 0}}^{\Delta_n} \bar{\bar{\boldsymbol{f}}}_{u_0}^{(h)\mathrm{H}} \bar{\bar{\boldsymbol{G}}}_n^{(h)} \boldsymbol{C}\boldsymbol{d}_{n_0+n} + \bar{\bar{\boldsymbol{f}}}_{u_0}^{(h)\mathrm{H}} \bar{\bar{\boldsymbol{v}}}_{n_0}. \end{aligned} \tag{16}$$

As can be seen, similar to (10), the estimated symbol includes four parts. The first part contains the u_0th data symbol at the n_0th time instant, which is desired. The second part contains the interference of other data symbols at the n_0th time instant on the desired symbol. The third part contains interference of other time instants on the desired symbol and the fourth part is noise. We try to obtain $\bar{\bar{\boldsymbol{f}}}_{u_0}^{(h)}$ that maximises SINR of the u_0th data symbol. To this end, by using (16) and considering that the transmitted symbols are independent and identically distributed (i.i.d) random variables with zero mean and power of one, power of the desired symbol ($P_{u_0}^{(\mathrm{d})}$), power of interference ($P_{u_0}^{(\mathrm{I})}$), and power of noise ($P_{u_0}^{(\mathrm{n})}$) for the u_0th data symbol at the n_0th time instant are calculated as

$$\begin{aligned} P_{u_0}^{(\mathrm{d})} &= \bar{\bar{\boldsymbol{f}}}_{u_0}^{(h)\mathrm{H}} \bar{\bar{\boldsymbol{G}}}_0^{(h)} \boldsymbol{c}_{u_0} \boldsymbol{c}_{u_0}^{\mathrm{T}} \bar{\bar{\boldsymbol{G}}}_0^{(h)\mathrm{H}} \bar{\bar{\boldsymbol{f}}}_{u_0}^{(h)}; \\ P_{u_0}^{(\mathrm{I})} &= \bar{\bar{\boldsymbol{f}}}_{u_0}^{(h)\mathrm{H}} \bar{\bar{\boldsymbol{A}}}_{u_0} \bar{\bar{\boldsymbol{f}}}_{u_0}^{(h)}; \\ P_{u_0}^{(\mathrm{n})} &= \bar{\bar{\boldsymbol{f}}}_{u_0}^{(h)\mathrm{H}} \bar{\bar{\boldsymbol{B}}} \bar{\bar{\boldsymbol{f}}}_{u_0}^{(h)}, \end{aligned} \tag{17}$$

where

$$\begin{aligned} \bar{\bar{\boldsymbol{A}}}_{u_0} &= \bar{\bar{\boldsymbol{G}}}_0^{(h)} \left(\sum_{\substack{u=1 \\ u\neq u_0}}^{U} \boldsymbol{c}_u \boldsymbol{c}_u^{\mathrm{T}} \right) \bar{\bar{\boldsymbol{G}}}_0^{(h)\mathrm{H}} \\ &\quad + \left(\sum_{\substack{n=-\Delta_n \\ n\neq 0}}^{\Delta_n} \bar{\bar{\boldsymbol{G}}}_n^{(h)} \boldsymbol{C}\boldsymbol{C}^{\mathrm{T}} \bar{\bar{\boldsymbol{G}}}_n^{(h)\mathrm{H}} \right) \end{aligned} \tag{18}$$

and $\bar{\bar{\boldsymbol{B}}} = \mathrm{E}\left[\bar{\bar{\boldsymbol{v}}}_{n_0} \bar{\bar{\boldsymbol{v}}}_{n_0}^{\mathrm{H}}\right]$ is the covariance matrix of the noise vector, which is a Hermitian matrix with the size of $MN_{\mathrm{R}} \times MN_{\mathrm{R}}$. According to (17), the SINR of the u_0th data symbol can be calculated as

$$\mathrm{SINR}_{u_0} = \frac{P_{u_0}^{(\mathrm{d})}}{P_{u_0}^{(\mathrm{I})} + P_{u_0}^{(\mathrm{n})}} = \frac{\bar{\bar{\boldsymbol{f}}}_{u_0}^{(h)\mathrm{H}} \bar{\bar{\boldsymbol{G}}}_0^{(h)} \boldsymbol{c}_{u_0} \boldsymbol{c}_{u_0}^{\mathrm{T}} \bar{\bar{\boldsymbol{G}}}_0^{(h)\mathrm{H}} \bar{\bar{\boldsymbol{f}}}_{u_0}^{(h)}}{\bar{\bar{\boldsymbol{f}}}_{u_0}^{(h)\mathrm{H}} \left(\bar{\bar{\boldsymbol{A}}}_{u_0} + \bar{\bar{\boldsymbol{B}}} \right) \bar{\bar{\boldsymbol{f}}}_{u_0}^{(h)}}. \tag{19}$$

As explained in [16, 25], vector $\bar{\bar{\boldsymbol{f}}}_{u_0}^{(h)}$ that maximise SINR_{u_0} is obtained as

$$\bar{\bar{\boldsymbol{f}}}_{u_0}^{(h)} = \left(\bar{\bar{\boldsymbol{A}}}_{u_0} + \bar{\bar{\boldsymbol{B}}} \right)^{-1} \bar{\bar{\boldsymbol{G}}}_0^{(h)} \boldsymbol{c}_{u_0}. \tag{20}$$

3.2 S2: separate beamforming after joint equalisation–despreading

In S2, as Fig. 3 shows, firstly, at each receiver antenna, despreading and equalisation are performed jointly as done for

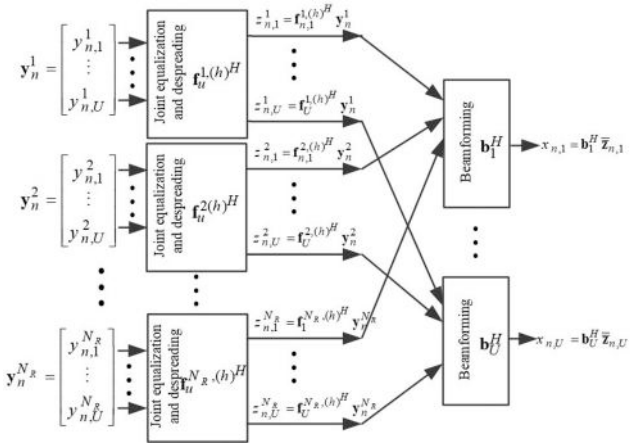

Fig. 3 *S2: separate beamforming after joint equalisation–despreading at the receiver of spread-OFDM/OQAM in SIMO channels*

SISO channels. Then, beamforming is performed on the resulted outputs of all antennas based on the information of all channels. Assume that the vector $\boldsymbol{f}_u^{l,(h)}$ with the length of M is applied at the lth receiver antenna for joint equalisation and despreading of the uth data symbol. By considering (13), the output of the joint equaliser and decoder of the u_0th data symbol at the l antenna is given as

$$\begin{aligned} z_{n_0,u_0}^{l} &= \boldsymbol{f}_{u_0}^{l,(h)\mathrm{H}}\boldsymbol{y}_{n_0}^{l} = \boldsymbol{f}_{u_0}^{l,(h)\mathrm{H}}\boldsymbol{G}_0^{l,(h)}\boldsymbol{c}_{u_0}d_{n_0,u_0} \\ &\quad + \boldsymbol{f}_{u_0}^{l,(h)\mathrm{H}}\boldsymbol{G}_0^{l,(h)}\sum_{\substack{u=1\\u\neq u_0}}^{U}\boldsymbol{c}_u d_{n_0,u} \\ &\quad + \sum_{\substack{n=-\Delta_n\\n\neq 0}}^{\Delta_n}\boldsymbol{f}_{u_0}^{l,(h)\mathrm{H}}\boldsymbol{G}_n^{l,(h)}\boldsymbol{C}\boldsymbol{d}_{n_0+n} + \boldsymbol{f}_{u_0}^{l,(h)\mathrm{H}}\boldsymbol{v}_{n_0}^{l}. \end{aligned} \tag{21}$$

Similar to the procedure considered for SISO channel and according to (10) and (11), $\boldsymbol{f}_{u_0}^{l,(h)}$ that maximises SINR of the u_0th data symbol at the n_0th time instant and the lth receiver antenna is obtained as

$$\boldsymbol{f}_{u_0}^{l,(h)} = \left(\boldsymbol{A}_{u_0}^{l} + \boldsymbol{B}^{l}\right)^{-1}\boldsymbol{G}_0^{l,(h)}\boldsymbol{c}_{u_0}, \tag{22}$$

where

$$\begin{aligned} \boldsymbol{A}_{u_0}^{l} &= \boldsymbol{G}_0^{l,(h)}\left(\sum_{\substack{u=1\\u\neq u_0}}^{U}\boldsymbol{c}_u\boldsymbol{c}_u^{\mathrm{T}}\right)\boldsymbol{G}_0^{l,(h)\mathrm{H}} \\ &\quad + \sum_{\substack{n=-\Delta_n\\n\neq 0}}^{\Delta_n}\boldsymbol{G}_n^{l,(h)}\boldsymbol{C}\boldsymbol{C}^{\mathrm{T}}\boldsymbol{G}_n^{l,(h)\mathrm{H}} \end{aligned} \tag{23}$$

and $\boldsymbol{B}^{l} = E\left[\boldsymbol{v}_{n_0}^{l}\boldsymbol{v}_{n_0}^{l\,\mathrm{T}}\right]$ is the covariance matrix of the noise vector at the lth receiver antenna with the size of $M\times M$. After joint equalisation–despreading, beamforming is performed on the decoded symbols of all antennas. We present the decoded symbols of the u_0th data symbol at the n_0th time instant for all antennas in a vector form as $\bar{\bar{\boldsymbol{z}}}_{n_0,u_0} \triangleq [z_{n_0,u_0}^{1} \quad \dots \quad z_{n_0,u_0}^{N_\mathrm{R}}]^{\mathrm{T}}$. By considering (21), $\bar{\bar{\boldsymbol{z}}}_{n_0,u_0}$ can be expressed as

$$\begin{aligned} \bar{\bar{\boldsymbol{z}}}_{n_0,u_0} &= \boldsymbol{q}_{0,u_0}^{(u_0)}d_{n_0,u_0} + \sum_{\substack{u=1\\u\neq u_0}}^{U}\boldsymbol{q}_{0,u}^{(u_0)}d_{n_0,u} \\ &\quad + \sum_{\substack{n=-\Delta_n\\n\neq 0}}^{\Delta n}\boldsymbol{Q}_n^{(u_0)}\boldsymbol{d}_{n_0+n} + \boldsymbol{w}_{n_0,u_0}, \end{aligned} \tag{24}$$

where $\boldsymbol{Q}_n^{(u_0)} = [\boldsymbol{q}_{n,1}^{(u_0)} \quad \dots \quad \boldsymbol{q}_{n,U}^{(u_0)}]$ is a $N_\mathrm{R}\times U$ matrix and $\boldsymbol{q}_{n,u}^{(u_0)} \triangleq [q_{n,u}^{1,(u_0)} \quad \dots \quad q_{n,u}^{N_\mathrm{R},(u_0)}]^{\mathrm{T}}$ is a vector with the length of N_R, in which the lth entry is $q_{n,u}^{l,(u_0)} = \boldsymbol{f}_{u_0}^{l,(h)\mathrm{H}}\boldsymbol{G}_n^{l,(h)}\boldsymbol{c}_u$. Also, $\boldsymbol{w}_{n,u} \triangleq [w_{n,u}^{1} \quad \dots \quad w_{n,u}^{N_\mathrm{R}}]^{\mathrm{T}}$ is the noise vector with the length of N_R, whose lth entry is $w_{n,u}^{l} = \boldsymbol{f}_u^{l,(h)\mathrm{H}}\boldsymbol{v}_n^{l}$. In this scenario after equalisation and despreading, beamforming is performed. Assume that the beamformer vector for the u_0th data symbol is $\boldsymbol{b}_{u_0}$ with the length of N_R. Therefore, the u_0th estimated symbol at the n_0th time instant becomes

$$\begin{aligned} x_{n_0,u_0} &= \boldsymbol{b}_{u_0}^{\mathrm{H}}\bar{\bar{\boldsymbol{z}}}_{n_0,u_0} \\ &= \boldsymbol{b}_{u_0}^{\mathrm{H}}\boldsymbol{q}_{0,u_0}^{(u_0)}d_{n_0,u_0} + \sum_{\substack{u=1\\u\neq u_0}}^{U}\boldsymbol{b}_{u_0}^{\mathrm{H}}\boldsymbol{q}_{0,u}^{(u_0)}d_{n_0,u} \\ &\quad + \sum_{\substack{n=-\Delta_n\\n\neq 0}}^{\Delta n}\boldsymbol{b}_{u_0}^{\mathrm{H}}\boldsymbol{Q}_n^{(u_0)}\boldsymbol{d}_{n_0+n} + \boldsymbol{b}_{u_0}^{\mathrm{H}}\boldsymbol{w}_{n_0,u_0}. \end{aligned} \tag{25}$$

Similar to (16), (25) has four parts. The first part contains the desired symbol, the second and third parts contain interference and the last part is noise. Power of the desired symbol, interference, and noise can be, respectively, calculated as

$$\begin{aligned} P_{u_0}^{(\mathrm{d})} &= \boldsymbol{b}_{u_0}^{\mathrm{H}}\boldsymbol{q}_{0,u_0}^{(u_0)}\boldsymbol{q}_{0,u_0}^{(u_0)\mathrm{H}}\boldsymbol{b}_{u_0}; \\ P_{u_0}^{(\mathrm{I})} &= \boldsymbol{b}_{u_0}^{\mathrm{H}}\boldsymbol{A}_{u_0}\boldsymbol{b}_{u_0}; \\ P_{u_0}^{(\mathrm{n})} &= \boldsymbol{b}_{u_0}^{\mathrm{H}}\boldsymbol{B}_{u_0}\boldsymbol{b}_{u_0}, \end{aligned} \tag{26}$$

where

$$\boldsymbol{A}_{u_0} = \sum_{\substack{u=1\\u\neq u_0}}^{U}\boldsymbol{q}_{0,u}^{(u_0)}\boldsymbol{q}_{0,u}^{(u_0)\mathrm{H}} + \sum_{\substack{n=-\Delta_n\\n\neq 0}}^{\Delta n}\boldsymbol{Q}_n^{(u_0)}\boldsymbol{Q}_n^{(u_0)\mathrm{H}} \tag{27}$$

and $\boldsymbol{B} = \mathrm{E}\left[\boldsymbol{w}_{n_0,u_0}\boldsymbol{w}_{n_0,u_0}^{\mathrm{H}}\right]$ is the covariance matrix of the noise vector $\boldsymbol{w}_{n_0,u_0}$ with the size of $N_\mathrm{R}\times N_\mathrm{R}$. Therefore, the SINR of the u_0th data symbol after beamforming is

$$\mathrm{SINR}_{u_0} = \frac{\boldsymbol{b}_{u_0}^{\mathrm{H}}\boldsymbol{q}_{0,u_0}^{(u_0)}\boldsymbol{q}_{0,u_0}^{(u_0)\mathrm{H}}\boldsymbol{b}_{u_0}}{\boldsymbol{b}_{u_0}^{\mathrm{H}}(\boldsymbol{A}_{u_0}+\boldsymbol{B}_{u_0})\boldsymbol{b}_{u_0}}. \tag{28}$$

By considering (19) and (20), as explained in [25], SINR_{u_0} in (28) is maximised when

$$\boldsymbol{b}_{u_0} = \left(\boldsymbol{A}_{u_0}+\boldsymbol{B}_{u_0}\right)^{-1}\boldsymbol{q}_{0,u_0}^{(u_0)}. \tag{29}$$

3.3 S3: separate equalisation, despreading, and beamforming

In the last scenario S3, in order to reduce the complexity, as Fig. 4 shows, at each antenna, firstly a one-tap per-subcarrier equaliser is used similar to that proposed in [14]. Then, despreading is performed without knowing the channel states by applying matrix $\boldsymbol{C}^{\mathrm{T}}$ to the equalised symbols. In the last step, similar to S2, beamforming is applied to the resulted outputs of all antennas based on the information of channel states. Assume that the

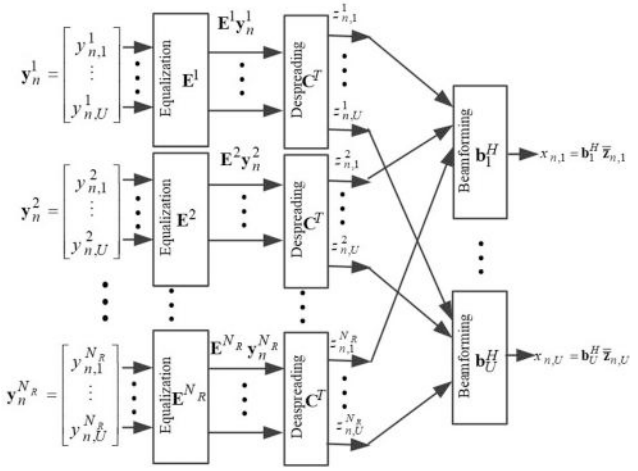

Fig. 4 *S3: separate equalisation, despreading and beamforming at the receiver of spread-OFDM/OQAM in SIMO channels*

Table 1 Parameters of the communication system in simulations

Parameter	Value/type
modulation	4-QAM
prototype filter	IOTA
carrier frequency	$f_c = 1\,\text{GHz}$
frequency shift step	$F_0 = 15\,\text{kHz}$
number of subchannels	$M = 256$
sampling period	$t_s = 1/MF_0 = 260\,\text{ns}$
time shift step	$T_0 = Mt_s/2 = 33,280\,\text{ns}$

diagonal matrix $\boldsymbol{E}^l$ is the equaliser matrix with the size of $M \times M$, which is used on the lth antenna and multiplied to $\boldsymbol{y}_n^l$ in order to eliminate the channel effect in the lth antenna at the nth time instant. After equalisation, by multiplying matrix $\boldsymbol{C}^{\mathrm{T}}$ to the resulted signals, all data symbols are despread as

$$\boldsymbol{z}_{n_0}^l = \boldsymbol{C}^{\mathrm{T}}\boldsymbol{E}^l\boldsymbol{y}_{n_0}^l, \tag{30}$$

in which $\boldsymbol{z}_{n_0}^l \triangleq [z_{n_0,1}^l \quad \dots \quad z_{n_0,u_0}^l]^{\mathrm{T}}$ and $z_{n_0,u_0}^l = \boldsymbol{c}_{u_0}^{\mathrm{T}}\boldsymbol{E}^l\boldsymbol{y}_{n_0}^l$. Similar to S2, in the following, in order to estimate the u_0th symbols at the n_0 th time instant, vector $\bar{\bar{\boldsymbol{z}}}_{n_0,u_0} \triangleq [z_{n_0,u_0}^1 \quad \dots \quad z_{n_0,u_0}^{N_{\mathrm{R}}}]^{\mathrm{T}}$ is organised for $u_0 = 1, 2, \dots, U$ and then beamforming is performed by multiplying $\boldsymbol{b}_{u_0}^{\mathrm{H}}$ into $\bar{\bar{\boldsymbol{z}}}_{n_0,u_0}$. Vector $\boldsymbol{b}_{u_0}$, which maximises SINR_{u_0}, is obtained as (29). Note that just in this case $q_{n,u}^{l,(u_0)} = \boldsymbol{c}_{u_0}\boldsymbol{E}^l\boldsymbol{G}_n^{l,(h)}\boldsymbol{c}_u$.

4 Complexity of the proposed scenarios

In this section, we compare the computational complexity of the three proposed scenarios. In S1 (joint equalisation–despreading–beamforming), the vector of coefficients for the u_0th data symbol ($\bar{\bar{\boldsymbol{f}}}_{u_0}^{(h)}$) is obtained from (20). As it can be seen, (20) includes some matrix additions, matrix multiplications, and a matrix inversion. The calculation complexity order of two matrix addition and multiplication with the size of $M \times M$ is, respectively, $O(M^2)$ and $O(M^{2.37})$. Also, the complexity of matrix inversion in general case is the same as matrix multiplication [26]. However, since the matrix, which must be inversed in (20), is symmetric positive definite, the complexity order of inversion of this matrix is much lower [27]. The size of all matrices in (20) is $MN_{\mathrm{R}} \times MN_{\mathrm{R}}$. Therefore, the overall calculation complexity order of this equation is $O((MN_{\mathrm{R}})^{2.37})$.

In S2, firstly, equalisation and despreading are performed jointly and then beamforming is applied. For the u_0th data symbol, the joint equaliser and despreader vector ($\boldsymbol{f}_{u_0}^{l,(h)}$) are calculated in (22). The size of all matrices in this equation is $M \times M$. Therefore, the calculation complexity order of this equation is $O(M^{2.37})$. The beamformer vector ($\boldsymbol{b}_{u_0}$) is calculated from (29). The size of all matrices in this equation is $N_{\mathrm{R}} \times N_{\mathrm{R}}$ and the complexity order becomes $O(N_{\mathrm{R}}{}^{2.37})$. Since the number of subcarriers (M) is considered very larger than the number of receiver antennas (N_{R}), it can be concluded that the calculation complexity of S2 is $O(M^{2.37})$, which is smaller than that of S1. When the number of receiver antennas is increased, this difference becomes larger.

In the last scenario (S3), equalisation, despreading, and beamforming are performed, separately. Also, equalisation at each subcarrier is performed independently from other subcarriers. Therefore, for each data symbol, the calculation complexity of equalisation (in all subcarriers) is $O(M)$. In S3, despreading code is the same spreading code applied in the transmitter. Thus, the receivers do not need to calculate the despreading codes. Beamforming is performed the same as S2. Therefore, the complexity order of beamforming is $O(N_{\mathrm{R}}{}^{2.37})$. Thus, the complexity order of the last scenario becomes $O(\max\{M, N_{\mathrm{R}}{}^{2.37}\})$. By comparing the complexity order of S2 and S3, it can be concluded that the calculation complexity of S3 is very smaller than that of S2.

We can compare the computational complexity of the proposed methods with OFDM in the SIMO channel as a benchmark. The computational complexity order of OFDM depends on the kinds of beamforming and equalisation methods used at each receiver antenna. Consider that at each receiver antenna a one-tap minimum mean square error (MMSE) equaliser is applied. Also, assume that fast Fourier transform algorithm is used for the calculation of the channel coefficient at each subcarrier. In this case, the computational complexity of OFDM for all antennas will be $O(N_{\mathrm{R}}M\log_2(M))$ [28].

5 Simulation results

In this section, we compare the performance of the proposed methods in terms of BER. Also, CP-OFDM and the proposed method in [13], (Zakaria method) performances in SIMO channels are evaluated. Simulation parameters are given in Table 1. The standard length of CP, which is considered here for CP-OFDM, is equal to 1/8 number of subcarriers ($(1/8) \times 256 = 32$) [29]. In CP-OFDM and Zakaria methods, at each receiver antenna, and at each subcarrier, an MMSE beamformer is used. The length of each data block and CP in the Zakaria method are considered 32 and 2, respectively. Also, for the last scenario proposed in this study (S3), in which all processes are performed separately, a one-tap MMSE equaliser is used at each subcarrier. In all simulations, we assume that the channel states are known perfectly, at the receiver.

In order to evaluate BER of the proposed scenarios, at first, we consider a frequency selective channel with the power delay profile (PDP) of pedestrian B, given as [30]

$$\begin{aligned}\text{Delays} &= [0 \quad 200 \quad 800 \quad 1200 \quad 2300 \quad 3700]\,\text{ns}.\\ \text{Powers} &= [0 \quad -0.9 \quad -4.9 \quad -8 \quad -7.8 \quad -23.9]\,\text{dB}.\end{aligned}$$

The pedestrian-B model generates high-frequency selective channels and can disclose the difference of the proposed methods in a very disruptive channel, which happens in 5G. In Fig. 5, the BER performance of the proposed scenarios, CP-OFDM and Zakaria method versus signal to noise ratio (SNR) are shown when a single antenna is used at the receiver ($N_{\mathrm{R}} = 1$). It can be seen that the performances of S1 and S2 are perfectly the same because when we have a single antenna, beamforming is not feasible and just equalisation and despreading must be applied, which in both S1 and S2 are performed, jointly. On the other hand, S1 and S2 outperform CP-OFDM, due to the fact that equalisation and decoding in the proposed methods are performed jointly and accordingly, these methods can remove the interference, very well. The BER performance of the last scenario is worse than CP-OFDM. It is because of that in S3, three operations of equalisation,

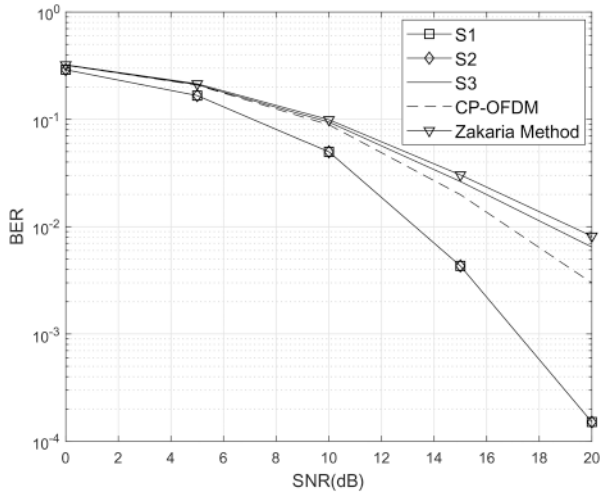

Fig. 5 *BER versus SNR for pedestrain-B channel when* $N_R = 1$

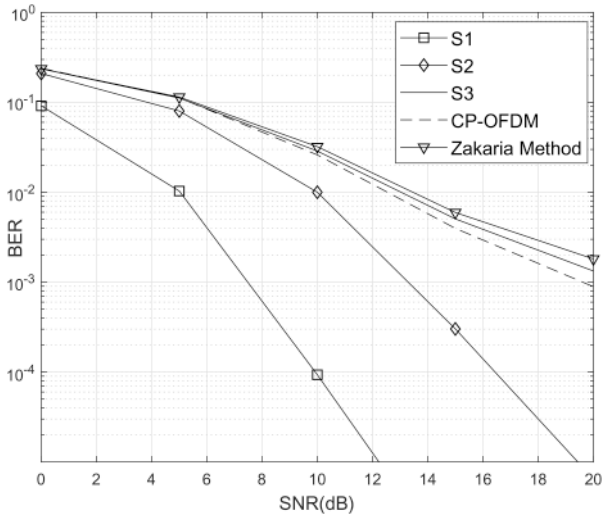

Fig. 6 *BER versus SNR for pedestrain-B channel when* $N_R = 3$

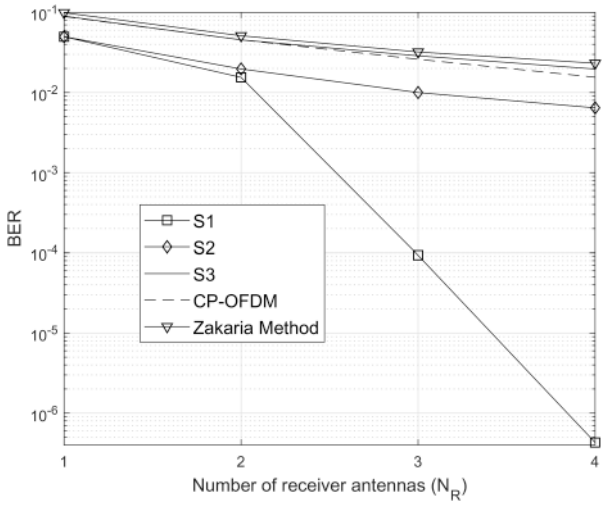

Fig. 7 *BER versus number of receiver antennas* (N_R) *for pedestrain-B channel when* SNR = 10 dB

despreading, and beamforming are done, separately. The maximisation of SINR at each step independently does not necessarily lead to maximisation of total SINR. In addition, since in the first step of S3, a single tap equaliser is employed, the interference caused by the channel cannot be perfectly removed. Therefore, in the second step, in addition to the inherent interference of the system, the channel interference also remains. On the other hand, in the second step of S3, despreading is done by

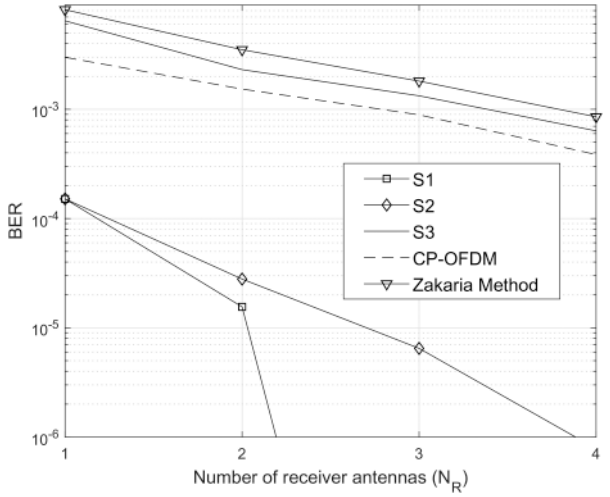

Fig. 8 *BER versus number of receiver antennas* (N_R) *for pedestrain-B channel when* SNR = 20 dB

using the same spreading code, which is applied at the transmitter, in order to remove inherent interference of system completely. Thus, it is concluded that the deaspreading operation cannot cancel both channel and inherent interferences. On the other side, in CP-OFDM, CP is used to prevent inter-block-interference, which improves performance.

In general, it must be noted that in the proposed methods, no CP is used and the bandwidth efficiency of spread-OFDM/OQAM is 100% while the bandwidth efficiency of CP-OFDM in these simulations is 89%. Also, we can see that in Fig. 5 that the proposed methods outperform Zakaria method. It is shown that the Zakaria method cannot perfectly cancel the interference in highly frequency selective channels.

Fig. 6 shows BER versus SNR when the number of receiver antennas is $N_R = 3$. It is seen that S1 significantly outperforms other methods. Actually, since all coefficients of equalisation, despreading and beamforming are obtained together in one step (based on the SINR maximisation), S1 is the optimised scenario among three proposed scenarios. After S1, S2 achieves better performance. Also, BER of S3 and CP-OFDM are approximately the same. Also, the Zakaria method achieves poorer performance compared to CP-OFDM.

In order to have a better comparison of the proposed scenarios, in Fig. 7, BER for a different number of receiver antennas is shown at SNR = 10 dB. This figure exhibits that by increasing the number of receiver antennas, the BER performance of all methods tends to be better. Obviously, the rate of BER reduction in S1 is very higher than that of other methods. It is noteworthy that although S1 achieves very good performance, its implementation requires more computational complexity.

Also, in Fig. 8, BER versus N_R is shown for SNR = 20 dB. The same results as Fig. 7 can be seen in this figure, but the difference between the proposed methods is more clear.

To have more insight on the BER performance of the proposed methods, let us consider vehicular-A channel with PDP is given as [30]

$$\text{Delays} = [0 \quad 300 \quad 700 \quad 1100 \quad 1700 \quad 2500]\,\text{ns}.$$
$$\text{Powers} = [0 \quad -1 \quad -9 \quad -10 \quad -15 \quad -20]\,\text{dB}.$$

Fig. 9 shows BER versus SNR when $N_R = 3$. Also, Figs. 10 and 11 show BER versus number of receiver antennas (N_R) when SNR = 10 and 20 dB, respectively. The result trends in Figs. 9–11 are the same as Figs. 6–8, respectively. These results indicate that the different condition of channels does not influence the performance of the proposed scenarios.

All in all, simulation results lead us to this conclusion that if SNR and the number of receiver antennas (N_R) are low, the performance of the three proposed methods is approximately the same. In this case, the method with lower complexity (S3) is the

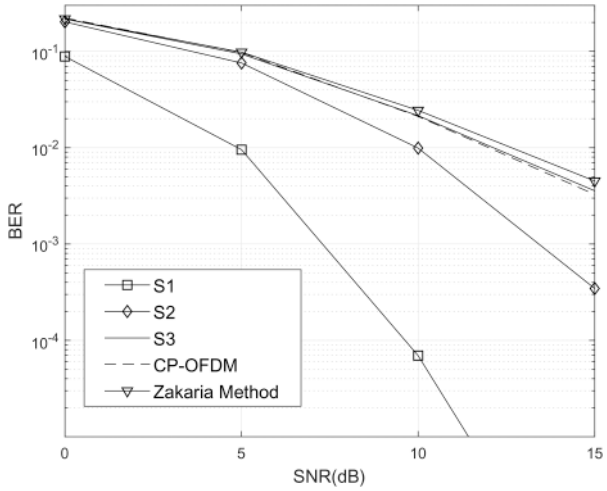

Fig. 9 *BER versus SNR for vehicular-A channel when* $N_R = 3$

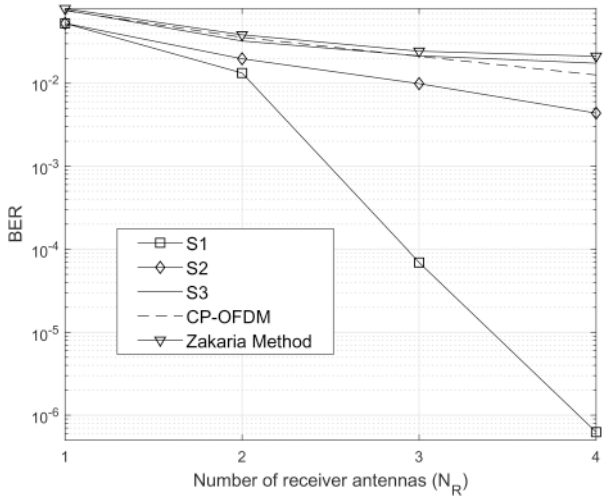

Fig. 10 *BER versus number of receiver antennas* (N_R) *for vehicular-A channel when* SNR = 10 dB

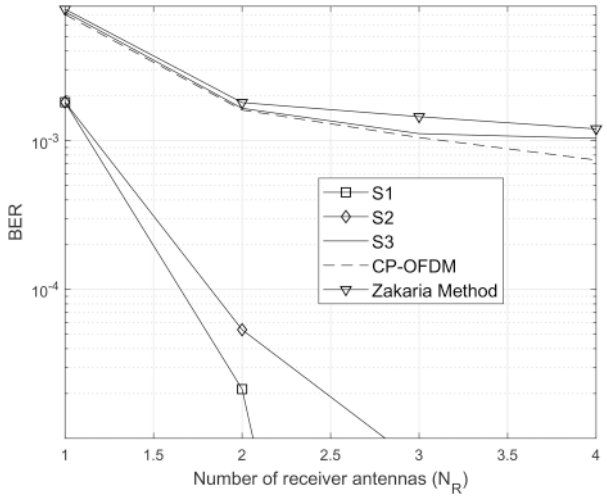

Fig. 11 *BER versus number of receiver antennas* (N_R) *for vehicular-A channel when* SNR = 20 dB

best method. By increasing N_R, when SNR is low, S1 achieves the best performance and if low complexity is not the primary demand, S1 is preferred. In this condition, S2 and S3 achieve the same performance, approximately. Thus, when low complexity is the main concern, S3 can be used. By increasing N_R and SNR, the performance of S1 is significantly better than S2, and the performance of S2 is superior to S3. Thus, in this case, if the priority is performance, such as broadcasting purposes, S1 is a better choice and when the matter of low complexity is considered, such as point to point communication, S2 is recommended. Generally, it can be said that there is a trade-off between complexity and performance, which by considering the application, an appropriate method can be selected.

6 Conclusion

In this study, we proposed three scenarios (S1, S2, and S3) for equalisation, despreading, and beamforming of complex spread-OFDM/OQAM when multiple antennas are applied at the receiver. In S1, all mentioned processes are jointly performed after demodulation in one step. Based on the SINR maximisation, we obtain an estimator vector, which is applied to the demodulated symbols of all antennas and all subcarriers at each time instant. In S2, at each antenna, equalisation and despreading are performed, jointly and after that, on the despread symbols of all antennas, beamforming is performed. The coefficients of the two steps are obtained subject to maximising SINR. In the last scenario (S3), the processes are performed, separately. Firstly, a one-tap equaliser is used at each subcarrier for each antenna. At the next step, spreading code, which is used at the transmitter, is applied at the receiver to despread the coded data symbols at each antenna. Finally, based on the SINR maximisation, beamforming is performed on the despread symbols of all antennas. S1 has the highest computational complexity and S3 has the lowest. Also, in simulations, it is shown that S1 has the best BER performance and S2 stands in the second place.

7 References

[1] Van Nee, R., Prasad, R.: '*OFDM for wireless multimedia communications*' (Arthec House, Boston, MA, 2000)

[2] IEEE Standard for Wireless LAN Medium Access Control (MAC) and Physical Layer (PHY) Specifications, IEEE 802.11 Standard, 1999

[3] Barhumi, I., Leus, G., Moonen, M.: 'Optimal training design for MIMO OFDM systems in mobile wireless channels', *IEEE Trans. Signal Process.*, 2003, **51**, (6), pp. 1615–1624

[4] Farhang-Boroujeny, B.: 'OFDM versus filter bank multicarrier', *IEEE Signal Process. Mag.*, 2011, **28**, (3), pp. 92–112

[5] Sahin, A., Guvenc, I., Arslan, H.: 'A survey on multicarrier communications: prototype filters, lattice structures, and implementation aspects', *IEEE Commun. Surv. Tutor.*, 2014, **16**, (3), pp. 1312–1338

[6] Farhang-Boroujeny, B., Moradi, H.: 'OFDM inspired waveforms for 5G', *IEEE Commun. Surv. Tutor.*, 2016, **18**, (4), pp. 2474–2492

[7] Rajabzadeh, M., Steendam, H.: 'Power spectral analysis of UW-OFDM systems', *IEEE Trans. Commun.*, 2018, **66**, (6), pp. 2685–2695

[8] Xu, K., Xu, Y., Ma, W., *et al.*: 'Time and frequency synchronization for multicarrier transmission on hexagonal time-frequency lattice', *IEEE Trans. Signal Process.*, 2013, **61**, (24), pp. 6204–6219

[9] Xu, K., Xu, Y., Zhang, D., *et al.*: 'On Max-SINR receivers for HMT systems over a doubly dispersive channel', *IEEE Trans. Veh. Technol.*, 2013, **62**, (5), pp. 2381–2387

[10] Saltzberg, B.: 'Performance of an efficient parallel data transmission system', *IEEE Trans. Commun. Technol.*, 1967, **15**, (6), pp. 805–811

[11] Asgari Tabatabaee, S.M.J., Zamiri-Jafarian, H.: ''Prototype filter design for FBMC systems via evolutionary PSO algorithm in highly doubly dispersive channels'', *Trans. Emerging Telecommun. Technol.*, 2017, **28**, (4), p. e3048

[12] Towliat, M., Asgari Tabatabaee, S.M.J.: 'On the time-frequency symbol density of FBMC/QAM systems', *Int. J. Commun. Syst.*, 2018, **31**, (6), p. e3516

[13] Zakaria, R., Le Ruyet, D.: 'A novel filter-bank multicarrier scheme to mitigate the intrinsic interference: application to MIMO systems', *IEEE Trans. Wirel. Commun.*, 2012, **11**, (3), pp. 1112–1123

[14] Lele, C., Siohan, P., Legouable, R., *et al.*: 'CDMA transmission with complex OFDM/OQAM', *EURASIP J. Wirel. Commun. Netw.*, 2008, **2008**, (1), p. 748063

[15] Lele, C., Siohan, P., Legouable, R.: 'The Alamouti scheme with CDMA-OFDM/OQAM', *EURASIP J. Adv. Signal Process.*, 2010, **2010**, (1), p. 703513

[16] Asgari Tabatabaee, S.M.J., Towliat, M., Samsami Khodadad, F.: 'Joint equalization-despreading method for OQAM-CDMA systems', *Signal Process.*, 2018, **146**, pp. 92–98

[17] Van Acker, K., Leus, G., Moonen, M., *et al.*: 'Per tone equalization for DMT-based systems', *IEEE Trans. Commun.*, 2001, **49**, (1), pp. 109–119

[18] Ikhlef, A., Louveaux, J.: 'Per subchannel equalization for MIMO FBMC/OQAM systems'. IEEE Pacific Rim Conf. on Communications, Computers and Signal Processing, University of Victoria, Victoria, B.C., Canada, August 2009, pp. 559–564

[19] Mestre, X., Majoral, M., Pfletschinger, S.: 'An asymptotic approach to parallel equalization of filter bank based multicarrier signals', *IEEE Trans. Signal Process.*, 2013, **61**, (14), pp. 592–606

[20] Asgari Tabatabaee, S.M.J., Zamiri-Jafarian, H.: 'Per-subchannel joint equalizer and receiver filter design in OFDM/OQAM systems', *IEEE Trans. Signal Process.*, 2016, **64**, (19), pp. 5094–5105
[21] Jungnickel, V., Manolakis, K., Zirwas, W*., et al.*: 'The role of small cells, coordinated multipoint, and massive MIMO in 5G', *IEEE Commun. Mag.*, 2014, **52**, (5), pp. 44–51
[22] Gao, Z., Dai, L., Mi, D*., et al.*: 'MmWave massive-MIMO-based wireless backhaul for the 5G ultra-dense network', *IEEE Wirel. Commun.*, 2015, **22**, (5), pp. 13–21
[23] Sengul, E., Akay, E., Ayanoglu, E.: 'Diversity analysis of single and multiple beamforming', *IEEE Trans. Commun.*, 2006, **54**, (6), pp. 990–993
[24] Vook, F.W., Ghosh, A., Thomas, T.A.: 'MIMO and beamforming solutions for 5G technology'. 2014 IEEE MTT-S Int. Microwave Symp. (IMS), Tampa, FL, USA, June 2014, pp. 1–4
[25] Asgari Tabatabaee, S.M.J., Zamiri-Jafarian, H.: 'Beamforming algorithms for multiuser MIMO uplink systems: parallel and serial approaches'. 21st Iranian Conf. on Electrical Engineering (ICEE), Mashhad, Iran, May 2013, pp. 1–5
[26] Le Gall, F.: 'Powers of tensors and fast matrix multiplication'. Proc. 39th Int. Symp. on Symbolic and Algebraic Computation, New York, NY, USA, July 2014, pp. 296–303
[27] Courrieu, P.: 'Fast computation of Moore–Penrose inverse matrices', 2008, arXiv preprint, arXiv:0804.4809
[28] Skinner, D.: 'Pruning the decimation in-time FFT algorithm', *IEEE Trans. Acoust. Speech Signal Process.*, 1976, **24**, (2), pp. 193–194
[29] Dobre, O.A., Venkatesan, R., Popescu, D.C.: 'Second-order cyclostationarity of mobile WiMAX and LTE OFDM signals and application to spectrum awareness in cognitive radio systems', *IEEE J. Sel. Top. Signal Process.*, 2012, **6**, (1), pp. 26–42
[30] Rec, I.T.U.R., ITU-R M. 1225: 'Guidelines for evaluation of radio transmission technology for IMT-2000', 1997, Technical Report